Simulative controller evaluation for an electro-hydrostatic excavator actuator with load-holding capability using active hysteresis and throttling control

Felix Figge, Katharina Schmitz

Institute for Fluid Power Drives and Systems (ifas), RWTH Aachen University, Aachen, Germany
E-mail: felix.figge@ifas.rwth-aachen.de, sc@ifas.rwth-aachen.de

Abstract

In recent years, the electrification of mobile machinery has progressed. Due to the change of the primary energy source, the hydraulic system must be more efficient and sustainable. In this context, the use of decentralized electro-hydrostatic actuators (EHA) is highly promising. Still, a widespread use cannot be observed. Reasons for this might be the higher initial component costs, worse dampening, as well as higher expenditure in the implementation of the required controls.

This paper presents a simulative evaluation of an electro-hydrostatic actuator with a hydraulic high-speed unit for use in mobile machinery. The circuit layout was selected based on cost considerations and includes load-holding capabilities. Furthermore, the load-holding valves are a key aspect of the control scheme. They are used to introduce a small active throttling at the discharge side of the cylinder in both pumping quadrants, thereby extending their load pressure range and enabling full operational coverage of the four-quadrants. The developed controller is mainly based on two state machines. It aims to synchronize the switching times of the valves with motor speed to enhance system performance and prevent system excitation. The controller is implemented in Matlab Simulink. For the aspired evaluation, it was coupled with a lumped parameter model of the circuit. The simulated cylinder velocities for several different speed and load combinations are evaluated to determine the control performance. Special focus is placed on the quadrant changes.

Keywords: EHA, four-quadrants, electrification, active throttling, hysteresis control

1 Introduction

In recent years, the electrification of mobile machinery has progressed. A wide range of electrified vehicles, including larger ones, is now available. The change of the prime mover from a combustion engine to an electric motor can be considered the most important change in mobile hydraulics of the past decades. Historically, many mobile machines use a centralized hydraulic pressure supply, which distributes the power via valves and fluid lines to the actuators. While this approach is cost-effective in terms of initial costs, it results in high valve throttle losses. These are mainly a result of the various actuators requiring different pressure levels. The recent focus on energy saving and the limited amount of energy available in machinery with batteries requires the hydraulic system to be more efficient and sustainable.

In this context, the use of decentralized electro-hydrostatic actuators (EHA) is highly promising. The use of a dedicated pump and motor for an actuator avoids the throttle losses from a higher to a lower pressure level. While EHAs are more often considered for industrial applications, widespread use in mobile machinery cannot be observed. Reasons for this might be the higher initial component costs, higher build volume, worse dampening, directly linked to the reduced system losses, as well as higher expenditure in the implementation of the required controls. The higher component costs of EHAs in comparison to a load-sensing system currently mainly arise from the additional prime movers as well as the additional hydraulic units. Furthermore, a decentralized hydraulic power supply with EHAs requires a small build volume to allow for easy integration into existing mobile machinery. An increase in rotational speed reduces the volume of the electric motor and allows the use of a pump with smaller displacement volume, reducing the total build volume of the EHA even further. Therefore, the underlying research project aims to develop a high-speed closed-circuit EHA for the application in mobile machinery.

Closed-circuit EHAs using a single pump are known to suffer from undesirable performance during certain operating conditions. Especially changes between operating quadrants are critical. Often, pressure feedback is used to increase the overall dampening of the system [1,2]. Williamson and Ivantysynova [3] developed a predictive observer to provide sufficient lead time for feed-forward control of pump displacement in a skid-steer and allow four-quadrant operation. The approach was aimed at dealing with excessive phase lag, rendering feedback control ineffective at handling mode-switching oscillations. They later concluded that the main problem is the interaction between mass and the compressible fluid that acts like a mass-spring-damper [1]. The unequal actuator areas aggravate any excitation because the pump still provides the same volume flow, sending the system back and forth between quadrants [1,2]. Increasing the system dampening is therefore recommended and pressure feedback is implemented. Michel further calculated a maximum allowable acceleration to prevent mode switches [2]. Wang et. al. [4] used electrically actuated proportional valves in combination with a control algorithm to introduce leakage in critical operation conditions for increased dampening and to prevent oscillation. The valves were added in addition to a shuttle valve. The compensation is only active close to critical operation conditions at low loads. They also use the valves to ensure the accumulator is connected to one cylinder side in case of oscillations of the shuttle valve. A mechanical variant of the added leakage in the critical region was presented by Çalışkan et. al. [5]. They used an underlapped shuttle valve, not requiring additional electrical valves, sensors and control algorithms. Imam et. al introduced a new valve type they called "limited throttling valve" to prevent oscillation in the critical region of a circuit using two POCV [6,7]. The valve is designed to restrict the cylinder flow only at low loads near the critical working conditions. Their simulation results show no oscillations in all operating conditions. They also show that the critical zone and oscillation amplitudes can be reduced by applying different charge pressures to both cylinder sides [7]. Costa and Sepehri [8] introduced a new four-quadrant definition based on the cylinder load pressure instead of the pressure difference over the pump. They concluded that this was the main reason for the poor behavior of earlier circuits. They also introduced a new circuit to account for their new quadrant definition. However, Gøytil et al. [9] showed that the proposed circuit can suffer from unwanted mode switches under certain conditions due to dynamic considerations. They suggest using an observer to calculate a modified force estimate to decide the valve states, eliminating the unwanted mode switches. The observer excludes forces introduced by valve switches and acceleration. Their strategy requires a certain accumulator pressure (in their case 30 bar) to prevent cavitation, which is inappropriate for certain circuits because of pressure limits. Their approach is software-based, while previous works primarily focused on hydraulic implementations. Kärnell and Ericson [10] investigated hysteresis control to prevent unwanted mode switches. They concluded that the pressures should be sensed in such a way that the difference is unchanged after a mode switch. Even then, switches can occur, but active hysteresis control reduces that risk if reservoir pressure is sufficient.

The approach presented in this paper uses the load pressure definition by [5,8] and implements active throttling [7,10] to allow full coverage of the four-quadrant plane in an excavator. Further, to reduce mode switches due to small pressure oscillations, active hysteresis is added [10]. The control approach further tries to minimize cylinder velocity spikes during quadrant changes by decoupling the cylinder from the pump by use of the incorporated load-holding valves.

Following, the selected circuit is introduced and its operation boundaries are derived. Afterwards, the developed control scheme is presented and validated by use of a lumped parameter simulation.

2 Circuit

There are many circuits for EHAs known in literature. An overview including a classification was introduced by Ketelsen et. al. [11]. Regarding the underlying project aiming to integrate the EHA into mobile machinery, especially excavators, the following restrictions excluded certain circuit layouts. In general, components with fewer and simpler parts cost less. Therefore, it was decided to use internal gear pumps with fixed displacement, which have fewer and simpler parts than piston pumps. Initially, circuits using more than one pump were considered to allow for a larger variety of layouts. The use of a fixed displacement hydraulic unit requires a variable speed prime mover for flow adjustment. Since variable speed prime movers are expensive, only one should be used. The EHA shall be encapsulated with only electrical and mechanical connections, requiring some sort of internal reservoir to store the differential fluid volume of the cylinder. The application in mobile machinery with uncertain operation conditions requires the capability to operate in all four quadrants. To achieve high efficiency, the EHA shall be capable of recuperating energy. Furthermore, the integration of load-holding valves was deemed to be necessary to allow a full stop of the prime mover and prevent overheating as well as wear on the hydraulic unit. Based on these restrictions, four circuits were selected for closer investigation. The circuits were introduced in [12] and are using a single fixed displacement pump with one exception. The first circuit uses pilot-operated check valves (POCV) to accommodate for the differential volume flow of the cylinder [13] as well as for load-holding [14]. The second circuit uses a cylinder with multiple chambers, allowing for a structural design close to a differential cylinder with equal rod and piston areas [15]. The differential volume flow is thereby omitted. The third circuit uses two pumps with a displacement ratio equal to the cylinder area ratio to provide appropriate volume flows [16]. The last circuit uses electrically actuated valves to handle the differential volume flow [9] as well as for load-holding. This circuit was selected for further investigation and will be regarded in the following sections

2.1 Selected circuit layout

The circuit shown in fig. 1 was selected because of the use of only a single hydraulic unit, the use of a standardized cylinder and the high customizability of the software control. The circuit mainly consists of the variable high-speed prime mover, a four-quadrant internal gear unit, as well as the differential cylinder. An accumulator is required to store the differential volume of the retracted cylinder rod length as well as to provide sufficient charge pressure for the hydraulic unit, especially at high speeds. To allow the differential flow to return to the accumulator, two electric switching valves $Diff_{rod}$ and $Diff_{pist}$ are included. They are called differential valves in the following. The electric actuation allows precise control over the timing of the connection between the pump ports and the accumulator. The load-holding valves LH_{rod} and LH_{pist} are designed to be proportionally adjusted. The oil flowing back into the accumulator is filtered using two additional check valves CV_{acc} and CV_{filter}. The check valves in parallel to the load-holding valves CV_{LH} and differential valves are required to prevent cavitation of the pump and the cylinder. During the circuit design, it was found that, based on available valves, separate oversized check valves were required to keep the pressure drop low enough to prevent cavitation. This was necessary because of the pressure level of the accumulator, which is limited to 10 bar because of the shaft sealing of the hydraulic unit. While an electric motor with a rotor running in oil can solve this by not needing a shaft seal, it introduces higher shear losses.

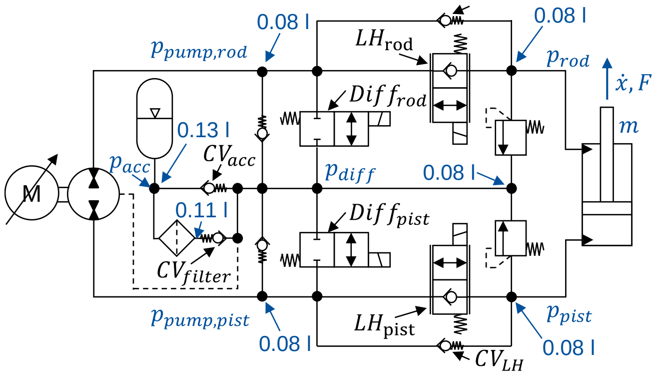

Figure 1: Circuit layout, pressures and fluid volumes

The operation of a cylinder can be divided into the well-known four-quadrants based on the cylinder velocity as well as the cylinder load, as shown in fig. 2. While the cylinder velocity is straightforward, different approaches for the load definition exist. They range from the pressure difference between the pump ports, the pressure difference between the cylinder chambers and the load pressure following eq. (1). In eq. (1) α represents the cylinder area ratio. The main advantage of the load pressure definition is the consideration of all active forces on the cylinder and only these forces, as can be seen in eq. (2). Therefore, the load pressure as defined by [5,8] is used as the second criterion for the quadrant definition. The external force F in fig. 2 is only used for clarification of load direction and does not represent the used criterion.

$$p_{load} = p_{pist} - \alpha \cdot p_{rod} \tag{1}$$

$$\begin{aligned} \ddot{x}m - F - F_{fric} &= p_{pist} \cdot A_{pist} - p_{rod} \cdot A_{rod} \\ &= p_{load} \cdot A_{pist} \end{aligned} \tag{2}$$

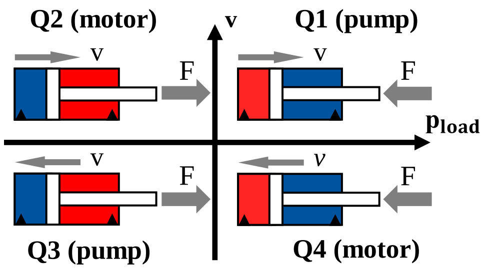

Figure 2: Four-quadrant plane

In fig. 3, the actuation of valves and oil flow in all four quadrants of operation is shown. Active valves are denoted with a green coil symbol and the oil flow with orange arrows. A simplified circuit layout with integrated check valves is used for clarity. Following the quadrant definition from fig. 2 the cylinder moves outwards in Q1 and Q2 (dark grey arrows) and in Q3 as well as Q4 inwards. Q1 and Q3 are the pumping quadrants in which the hydraulic unit is supplying energy into the circuit, marked with a light blue arrow towards the hydraulic unit. In Q2 and Q4 the unit works as a motor and extracts energy. Quadrant changes based on a reversal of cylinder movement (Q1↔Q4 or Q2↔Q3) are controlled by a change of motor speed and can therefore be more easily handled by the control scheme.

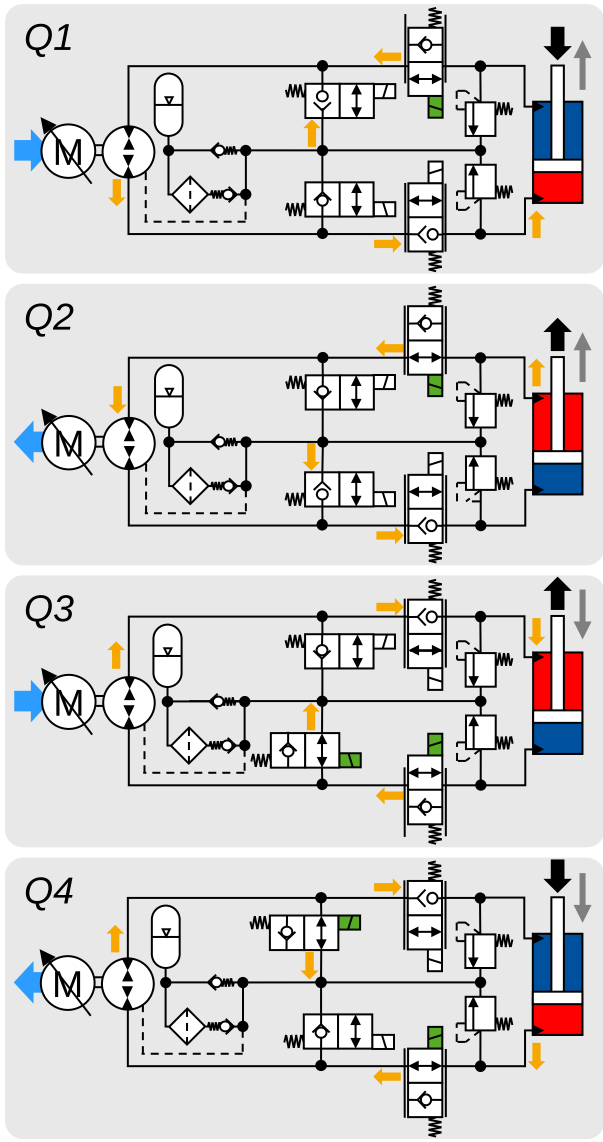

Figure 3: Valve actuation and oil flow in all four quadrants

A change of operating quadrant based on a direction reversal of the external load (Q1↔Q2 or Q3↔Q4) is more difficult. The exact time of direction change cannot be predicted. In both cases, it requires a change of motor speed because of the different cylinder areas. The speed change ideally should happen instantaneously but is limited by motor torque and inertia. The positions of the load-holding valves need to be adjusted as well. Additionally, for the changes between Q3 and Q4, a change of differential valve actuation is required, as can be seen in fig. 3. To avoid poor system performance due to unwanted system states, the valve actuation must be synchronous to the motor speed change.

Before going into detail about how these challenges were tackled, the circuit behavior is explained in more detail and the existing boundaries of operation are derived.

2.2 Circuit behavior and boundaries

A similar concept to the one in this section was investigated in [6] for a circuit without load-holding valves and differential flow handling by pilot-operated check valves.

First, the effect of the accumulator pressure is investigated. Neglecting all pressure drops across valves as well as all other forces, the accumulator pressure results in an active pushing force on the cylinder rod. The cylinder is moving outwards without energy input from the pump, corresponding to an operation in Q2. The related load pressure results by inserting the accumulator pressure p_{acc} into eq. (1) for both cylinder pressures (eq. (3)).

$$p_{bound,acc} = p_{acc} \cdot (1 - \alpha) \tag{3}$$

$p_{bound,acc}$ is larger than zero for all accumulator pressures larger than zero and thereby represents a new boundary between motor and pump operation. This can be checked for the other quadrant boundaries by considering an external force that pushes the cylinder inwards. The cylinder will only move inwards without assistance from the pump (Q4) if the external force is larger than the outwards pushing force from the accumulator pressure. This in turn would result in a load pressure that is larger than $p_{bound,acc}$, since p_{pist} would rise. The new boundary is shown in fig. 4 as a blue rectangle for an accumulator pressure between 4.6 bar and 10 bar, since the accumulator pressure changes during charging and discharging.

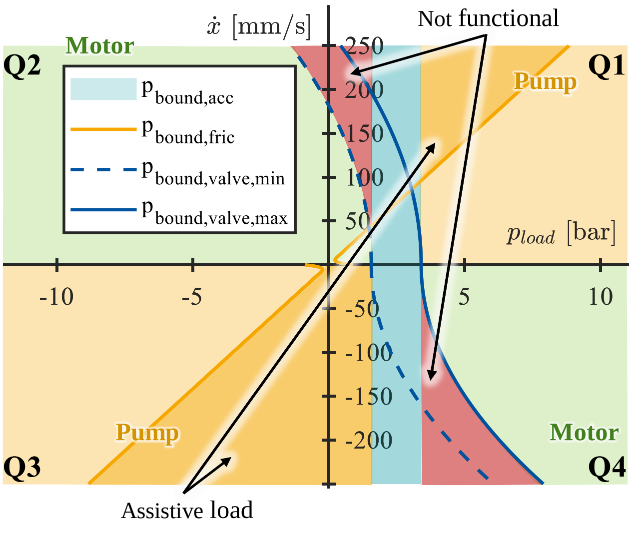

Figure 4: Load pressure boundaries of the circuit

Next, the quadrants Q1 and Q3 are considered, in which the pump provides power. If the pressure drop across the load-holding valves is neglected, stationary movement of the cylinder is assumed and no external force is applied, the load pressure originates only from the cylinder friction (see eq. (2)). The neglection of the pressure drop across the valves is not strictly necessary. A pressure increase on the discharging cylinder side due to the valve resistance would be canceled out in the load pressure calculation by the necessary pressure increase on the inflow side due to the force balance. Except for an increase in pump pressure, this has no further implications. The load pressure required for motion with a specific velocity $p_{bound,fric}$ follows from eq. (4) in Q1 and (5) in Q3 for load-free condition. The corresponding boundaries are drawn in orange in fig. 4 and are calculated by means of the friction model used in the simulation as defined by eq. (6) and the parameters given in tab. 1.

$$p_{bound,fric,Q1} = \frac{|F_{fric}|}{A_{pist}} \tag{4}$$

$$p_{bound,fric,Q3} = -\frac{|F_{fric}|}{A_{pist}} \tag{5}$$

$$\begin{gathered} F_{fric} = \begin{cases} F_{fric,base} + \mu_{vis} \cdot \dot{x} + F_{fric,mix} & , \ \dot{x} \leq \dot{x}_{vis} \\ F_{fric,base} + \mu_{vis} \cdot \dot{x} & , \ \dot{x} > \dot{x}_{vis} \end{cases} \\ F_{fric,mix} = \left(F_{fric,static} - F_{fric,base}\right) \cdot \left(1 - \frac{|\dot{x}|}{\dot{x}_{vis}}\right)^4 \end{gathered} \tag{6}$$

If the external force is pushing in Q1 and therefore has a negative sign, the load pressure will be higher than in the load-free condition, as stated by eq. (7). Therefore, a load pressure below the load-free condition can only be achieved if the external force assists the motion. The same conclusion can be made for Q3 by using eq. (8) with the only difference that an assistive load results in a higher load pressure due to the reversed movement direction. Both areas are marked in a darker orange shade in fig. 4. The boundary thereby can be used to determine if the external force is assistive, provided the friction force is known with sufficient accuracy. The only implication function-wise is that the load pressure will increase along the boundary line if the velocity is increased and no assistive load is applied. All the velocities inside the quadrant can still be achieved.

$$\begin{gathered} 0 \leq -F = p_{load} \cdot A_{pist} - |F_{fric}| \\ \Rightarrow p_{load} \geq \frac{|F_{fric}|}{A_{pist}} \end{gathered} \tag{7}$$

$$\begin{gathered} 0 \geq -F = p_{load} \cdot A_{pist} + |F_{fric}| \\ \Rightarrow p_{load} \leq -\frac{|F_{fric}|}{A_{pist}} \end{gathered} \tag{8}$$

Lastly, the quadrants with motor operation are investigated. Contrary to the previous case, energy is now provided by the cylinder and not the pump. The volume flow through the load-holding valves can be described by the orifice equation (9), which is further related to the cylinder velocity by eq. (10) considering the currently loaded cylinder side. $A^*(s)$ is the active flow area depending on the valve position s. One can directly conclude that the cylinder velocity will be limited for low pressure differences and therefore small external loads.

$$Q = \alpha_D \cdot A^*(s) \cdot \sqrt{2/\rho} \cdot \sqrt{\Delta p} = K(s) \cdot \sqrt{\Delta p} \quad (9)$$

$$\dot{x} = \frac{Q}{A_{pist/rod}} = \frac{K(s) \cdot \sqrt{\Delta p}}{A_{pist/rod}} \quad (10)$$

Therefore, the cylinder velocity will not be controlled by the rotational speed of the pump but by the orifice flow at low loads. The pressure at the pump inlet port will then be close to the accumulator pressure p_{acc} because the connected check valve opens to prevent cavitation. The pump outlet pressure is also close to p_{acc} because the corresponding differential valve is actuated and connects to the accumulator. Further, the unloaded cylinder chamber pressure is also at the same level because the check valve opens to prevent cavitation. Depending on the operating quadrant, the loaded cylinder side changes, resulting in eq. (11) for Q2 and eq. (13) for Q4 to calculate the boundary load pressure $p_{bound,valve}$ following the explanations beforehand. By rearranging eq. (11) and (13) to eq. (12) and (14) a relation between the pressure drop Δp and $p_{bound,valve}$ is derived. The second half of eq. (12) and (14) is equal to $p_{bound,acc}$, resulting in a dependence on the accumulator pressure. By inserting eq. (12) and (14) into eq. (10) a correlation between cylinder velocity and load pressure is derived, which is shown in fig. 4 as blue lines. These lines mark the needed load pressure $p_{bound,valve}$ to achieve the respective cylinder velocity. The solid line results for the maximum and the dashed line for the minimum accumulator pressure. If the load pressure falls "below" the current boundary, taking into consideration the different signs in Q2 and Q4, the velocity will sink along the boundary.

$$p_{bound,valve,Q2} = p_{acc} \qquad - \alpha \cdot (p_{acc} + \Delta p) \quad (11)$$

$$\Delta p_{Q2} = -\left[p_{bound,valve} - (1-\alpha) \cdot p_{acc}\right] \cdot 1/\alpha \quad (12)$$

$$p_{bound,valve,Q4} = p_{acc} + \Delta p - \alpha \cdot (p_{acc} \qquad) \quad (13)$$

$$\Delta p_{Q4} = +\left[p_{bound,valve} - (1-\alpha) \cdot p_{acc}\right] \quad (14)$$

In conclusion, an operation in motor mode is only possible above the boundary. The corresponding velocities and load pressures are marked green in fig. 4. By closer inspection, two areas between $p_{bound,acc}$ and $p_{bound,valve}$ remain, marked red in fig. 4, in which an operation of the circuit is not possible. The assistive load is not large enough to achieve the required volume flow through the load-holding valve and the cylinder velocity remains too low. Valves with smaller pressure drops reduce the area but do not remove the boundary completely. This behaviour is unacceptable for the operation in mobile machinery since it would result in a large and prolonged deviation from the control signal.

An extension of Q1, respectively Q3, and therefore the supply of energy from the pump in only these areas is theoretically possible. It requires the throttling of the cylinder discharge to allow the pump to control the cylinder velocity by providing volume flow in the otherwise unloaded cylinder chamber. Without the throttling, the cylinder would accelerate due to the external load. The valve characteristics need to be known precisely for this approach, which they generally are not. Further, they change during operation, for example, due to temperature. Assuming the control supposes a pressure drop that is too high, this would result in a larger volume flow near the boundary than expected. If the load pressure lies inside the red area. the pump would be providing energy by pumping into the cylinder. The higher discharge from the cylinder would result in a higher speed. There are only two ways to slow down the cylinder in this scenario. One would need the hydraulic unit to be working in motor mode and use it to control the cylinder velocity. This contradicts the earlier assumption that the unit is pumping. Secondly, the pressure drop across the valve could be increased to lower the volume flow out of the cylinder. Since the valve characteristics are not known precisely enough, as supposed at the beginning, a closed-loop control would be required. The required position sensor would increase the cost of the EHA and therefore, this approach was discarded.

If an extension of the pumping quadrants further than the red marked areas is allowed, a simpler approach, following the same principle, is possible. The valve is not actuated to match the pressure drop to the currently required volume flow, but to achieve a fixed pressured rop. This was discussed in [10] as a possible way to introduce hysteresis to prevent unwanted quadrant changes and was called "active throttling". No further investigation was carried out. A familiar approach was also introduced in [7] as "selective throttling" with specifically designed valves that increase throttling in the critical region to reduce oscillations. As was discussed, active throttling is needed to allow the investigated circuit with load-holding valves to cover the full operational range and not to introduce hysteresis or reduce oscillations. The fixed pressure drop must be larger than the pressure drop of the load-holding valves at the highest volume flow and full opening. Otherwise, the required volume flow at high cylinder velocity cannot be achieved. The fixed pressure drop results in a larger area in which the hydraulic unit can be operated in pumping mode without loss of control over the cylinder velocity. The new boundaries are calculated by eq. (15) for Q1 and eq. (16) for Q3. Exactly at these boundaries, the external load accelerates the cylinder and the volume flow provided by the pump becomes insufficient. The check valve opens to prevent cavitation, resulting in a pressure level close to p_{acc}. The pressure in the other cylinder chamber at the boundary equals p_{acc} plus the artificial pressure difference $\Delta p_{throttle}$. Again, the accumulator boundary $p_{bound,acc}$ is part of the equations resulting in a maximum and minimum boundary drawn as green lines in fig. 5 for $\Delta p_{throttle}$ set to 22 bar. While a reduction of $\Delta p_{throttle}$ above $p_{bound,acc}$ is possible, this is discarded to allow for better cylinder control.

$$\begin{aligned} &p_{pist} = p_{acc}\,; \qquad p_{rod} = p_{acc} + \Delta p_{throttle} \\ &\Rightarrow p_{bound,throttle,Q1} = p_{acc} \cdot (1-\alpha) - \alpha \cdot \Delta p_{throttle} \end{aligned} \quad (15)$$

$$\begin{aligned} &p_{pist} = p_{acc} + \Delta p_{throttle}\,; \qquad p_{rod} = p_{acc} \\ &\Rightarrow p_{bound,throttle,Q3} = p_{acc} \cdot (1-\alpha) + \Delta p_{throttle} \end{aligned} \quad (16)$$

The required control current to actuate the valve is taken from a characteristic diagram including the pressure difference, volume flow and current. The volume flow is calculated from the requested cylinder velocity. The boundary position is influenced by the accumulator pressure, which could be compensated for via measurement. Still, the characteristic diagram in general will be inaccurate and deviations are unavoidable. By introducing a virtual boundary below $p_{bound,throttle}$ and above $p_{bound,valve}$ a safety gap can be introduced to account for deviations. Additionally, "active hysteresis" [10] is added to this switching boundary so that small changes in load pressure will not result in a change of detected quadrant. The introduced hysteresis Δp_{Hyst} is drawn in violet in fig. 5 with a width of 4 bar. For a positive cylinder velocity, the motor mode in Q2 starts if the load pressure is below -10 bar. Afterwards, the EHA will change back to pump mode (Q1) only if the load pressure increases above -6 bar. Negative load pressures are the result of higher pressures on the rod side as defined by eq. (1).

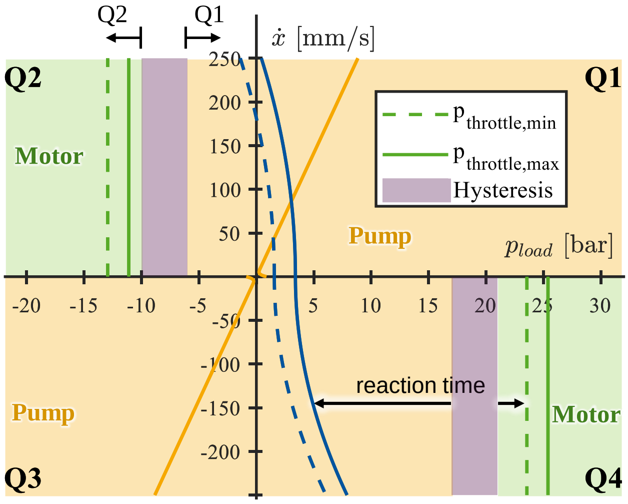

Figure 5: Load pressure boundaries of the circuit with active throttling and hysteresis

The positioning of the virtual boundary, including hysteresis, determines the amount of time before control of cylinder velocity is lost. These reaction times are exemplary marked in fig. 5 for Q4. For Q4→Q3 this timeframe starts when the load pressure falls below the left hysteresis boundary and ends when it reaches the valve boundary, since then the cylinder will start to slow down. The hysteresis boundary is not positioned in the middle because the control was developed for the arm of an excavator. Changes from Q1→Q2, as well as Q3→Q4, are unlikely during normal operation since the mass centre cannot cross the top centre position. The position of the virtual boundary and the width of the hysteresis are therefore dependent on the application and need to consider reaction time against the tendency of unwanted quadrant changes.

3 Control scheme

Based on the load pressure boundaries shown in fig. 5 a control scheme was implemented. The top level of the control is shown in fig. 6. The main component is the EHA controller that outputs the valve modes and required rotational speed depending on the loaded cylinder side. The speed request is limited and then adjusted by pressure feedback to reduce pressure oscillation [2]. Depending on the loaded cylinder side, one of the speed requests is fed into the characteristic field of the hydraulic unit, adjusted to compensate for volumetric losses and then output to the motor controller. The valve controllers output the current to actuate the load-holding valves based on different modes that are explained later. To reduce the number of pressure sensors p_{Diff} is used as the low-pressure level of the hydraulic unit, since the check valve is sized to have a low pressure drop. For clarity, the overload protection was left out, which increases the pressure drop over the load-holding valves during motor operation if the electric motor gets close to its torque limit. This is essential at high speeds to prevent an uncontrolled acceleration of the cylinder, since any acceleration reduces the torque capacity further.

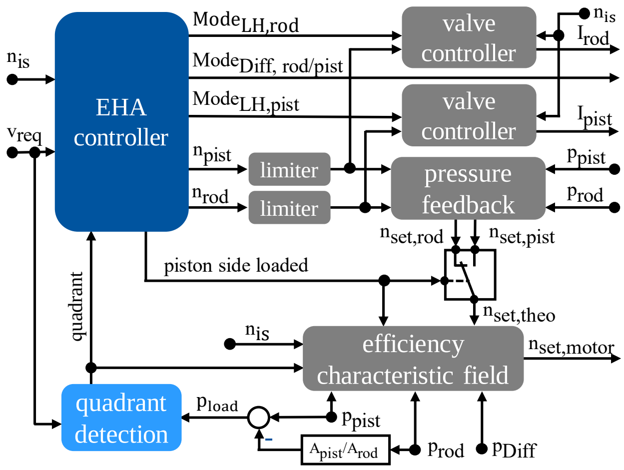

Figure 6: Top level of control scheme

The load pressure boundaries from fig. 5 are mainly implemented in the state machine for quadrant detection, as shown in fig. 7. In addition to the well-known four-quadrants, a fifth is added for the standstill of the EHA.

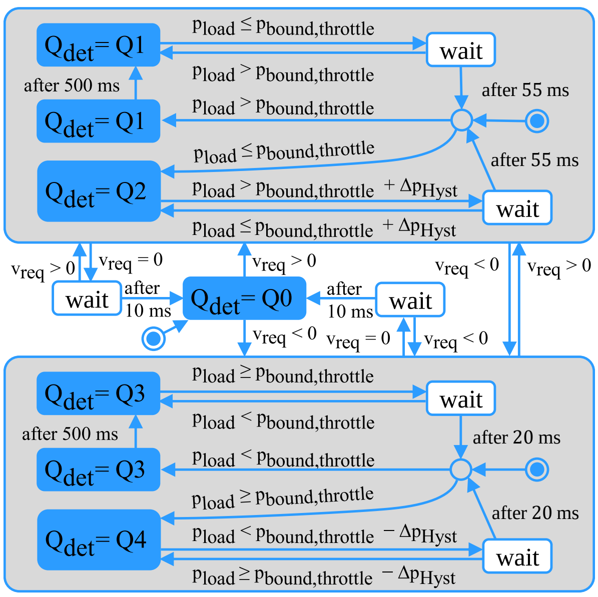

Figure 7: Quadrant detection

Based on the velocity request v_{req}, one of the substates is activated. Inside the substates the hysteresis boundaries for the load pressure p_{load} are implemented. To further prevent unwanted quadrant changes because of short impulses, additional wait times are introduced before a quadrant is left. A longer wait time of 500 ms is added after entering each of the pumping modes to allow the initial excitation after valve actuation to subside and to prevent a quadrant change. Therefore, the states in which Q1 and Q3 are detected are duplicated. The times are chosen based on iterative testing and might not be optimal. It shall be pointed out that a request to change velocity direction or to stop will still lead to a quick change of quadrant.

Following, the EHA controller state machine is introduced, whose main function is the synchronisation of the valve positions and motor speed. For example, before the pump starts to provide volume flow into the cylinder, the load-holding valve on the discharging cylinder side needs to be opened. There is a delay or dead time before a control signal change takes effect, which must be accounted for to achieve better system performance. The symbols used are explained in more detail in the nomenclature. They comprise the times needed to change valves states, the time delay of the motor $t_{dead,Motor}$, the current rotational speed of the hydraulic unit n_{is} and of course the detected quadrant Q_{det}.

Figure 8 shows the sequences for acceleration and reversal of the cylinder velocity. Based on the detected quadrant Q_{det} different sequences are necessary for acceleration. If the external load is directed against the requested movement direction (Q1 & Q3), first, the load-holding valve blocking the discharge of the cylinder is opened completely ("1") as well as the differential valve on the piston side in case of Q3. After the maximum switching time minus the motor delay has elapsed, the motor signal is applied. After a wait time equal to the motor delay, the valve on the outlet is then changed to throttling mode. The valve is first fully opened to prevent hydraulic tensioning of the cylinder. If an assistive load acts on the cylinder, a quick opening of the load-holding valves would result in a strong acceleration because of the sudden drop of pressure in the cylinder chamber. Afterwards the volume surplus due to the higher cylinder velocity would result in a pressure spike at the motor inlet slowing the cylinder down again. This behaviour was deemed to be unwanted and the displayed approach implemented. By briefly turning the hydraulic unit in the opposite direction the volume between the motor inlet and LH valve is pressurized. The approach could be refined further by adapting the time the pump turns depending on the pressure level. Additionally, the valve current is increased slowly ("opening") to allow for smoother pressure equalization and acceleration of the cylinder. As soon as the valve should start to move, after $t_{dead,LH}$ passed, the pump direction is changed back to the correct one. After stopping the cylinder, which is explained later, it is possible that the rotational unit is still spinning. To prevent the start of the sequences with a high-speed rotation in the wrong direction, a check against a threshold n_{wait} was added.

The reversal of the cylinder movement under the same load direction can be handled well by the controller since it is mainly influenced by the rotational speed of the hydraulic unit. But especially when entering the motoring quadrants Q2 & Q4, a precise synchronisation is required to prevent the earlier described pressure drop because of the motor turning while the valve is still closed. The implemented approach is compatible

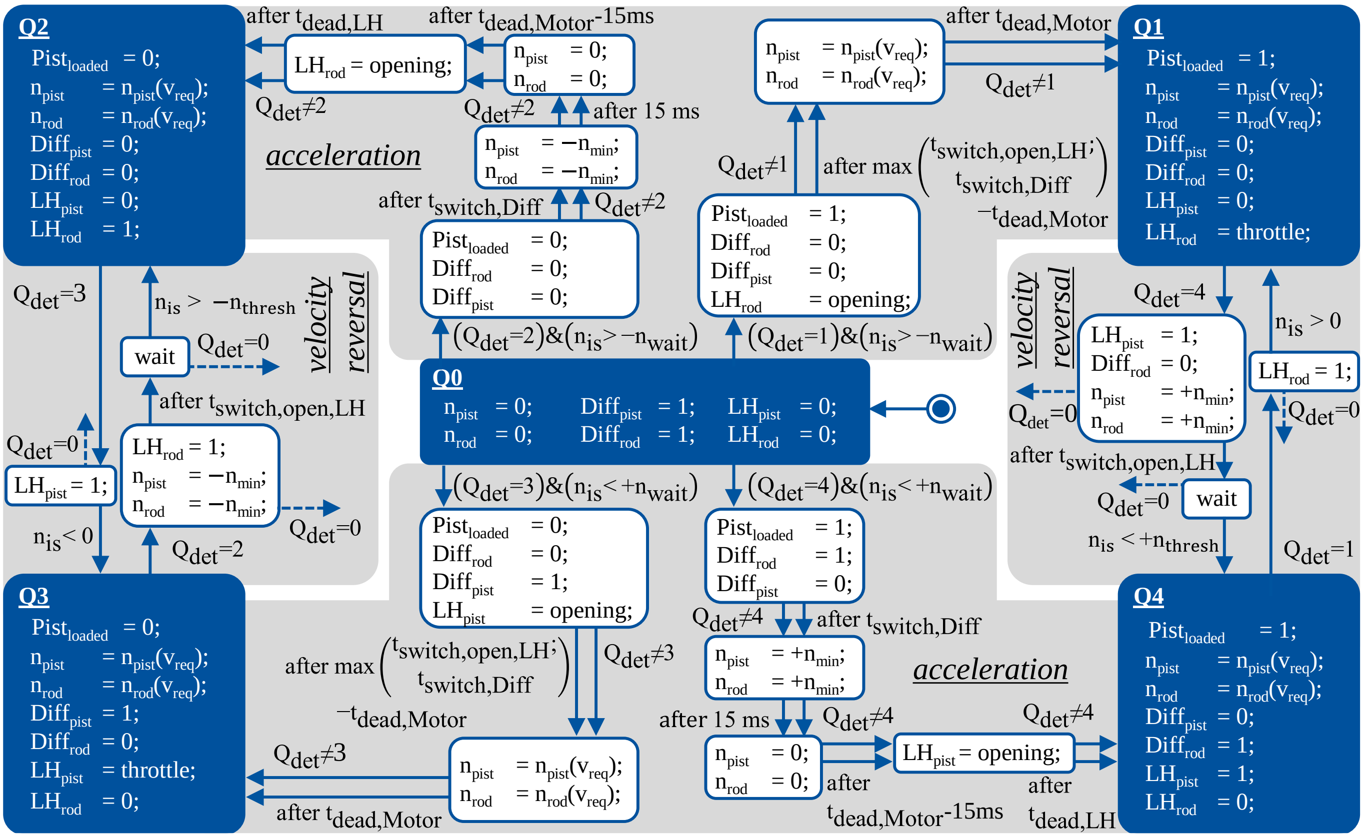

Figure 8: EHA controller – acceleration and reversal of cylinder movement

with either faster valve or motor characteristics as displayed in fig. 9. By first dropping the requested motor signal down to the minimum rotational speed n_{min} the speed is reduced, but a change of direction is prevented. Only after the switching time of the valve has passed, the signal is changed to the value calculated based on the requested speed, ensuring an open valve and preventing a pressure drop due to insufficient flow out of the cylinder. Further, the valve on the previous discharging side during pumping mode is only closed after the rotational speed drops below a certain threshold n_{thresh} ensuring that the pump has changed rotational direction and preventing a blockage of discharge.

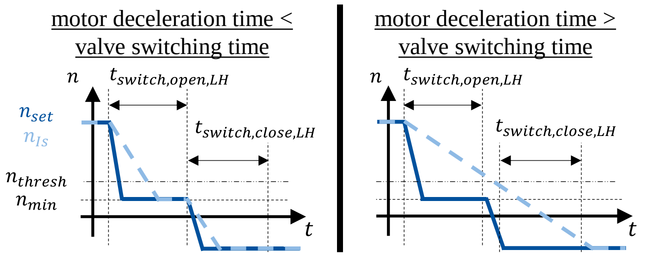

Figure 9: Motor speed request during movement reversal

A trivial value for n_{thresh} would be zero, but a higher value, considering the required switching time, can increase performance by earlier actuation. A change into the pumping quadrants requires less synchronisation because throttling and therefore hydraulic tensioning is desired. Depending on valve and motor characteristics, a more detailed synchronisation might be needed as well.

In fig. 10 the sequences for changing quadrant due to reversal of load direction and stopping are presented. Changes of load direction cannot be predicted and are critical since the loaded cylinder side changes, requiring an adaptation of the pump speed. As explained earlier, the time until a loss of control depends on the virtual boundary, the valve boundary and the throttle boundary. To allow for an adaptation of pump speed during the changes, the load-holding valves are switched to “resistance” mode. The cylinder speed in this mode is controlled by the valve using its characteristic map and the cylinder decoupled from the hydraulic unit.
If the change goes into a motoring quadrant, the valve is slowly opened for smooth pressure equalisation afterwards. To prevent the cylinder from being slowed down during Q3→Q4 the differential valve on the piston side is only closed if the difference between current and requested pump speed is smaller than 15% or after a time limit of 300 ms. The same logic is true for the change Q4→Q3 where the differential valve must open to prevent the reduction in rotational speed, slowing down the cylinder. The change Q2→Q1 only requires a change of the mode of the load-holding valve on the rod side. The time required for the increase of the pump speed depends on the motor performance and current load but is generally short. While the motor speed is too small, the cylinder velocity might be as well.

The implemented approaches will not result in a completely smooth cylinder velocity during changes but shall limit the intensity and duration of deviations as much as possible. The assessment of whether the remaining deviations can be accepted mainly depends on the subjective feel of the operator.

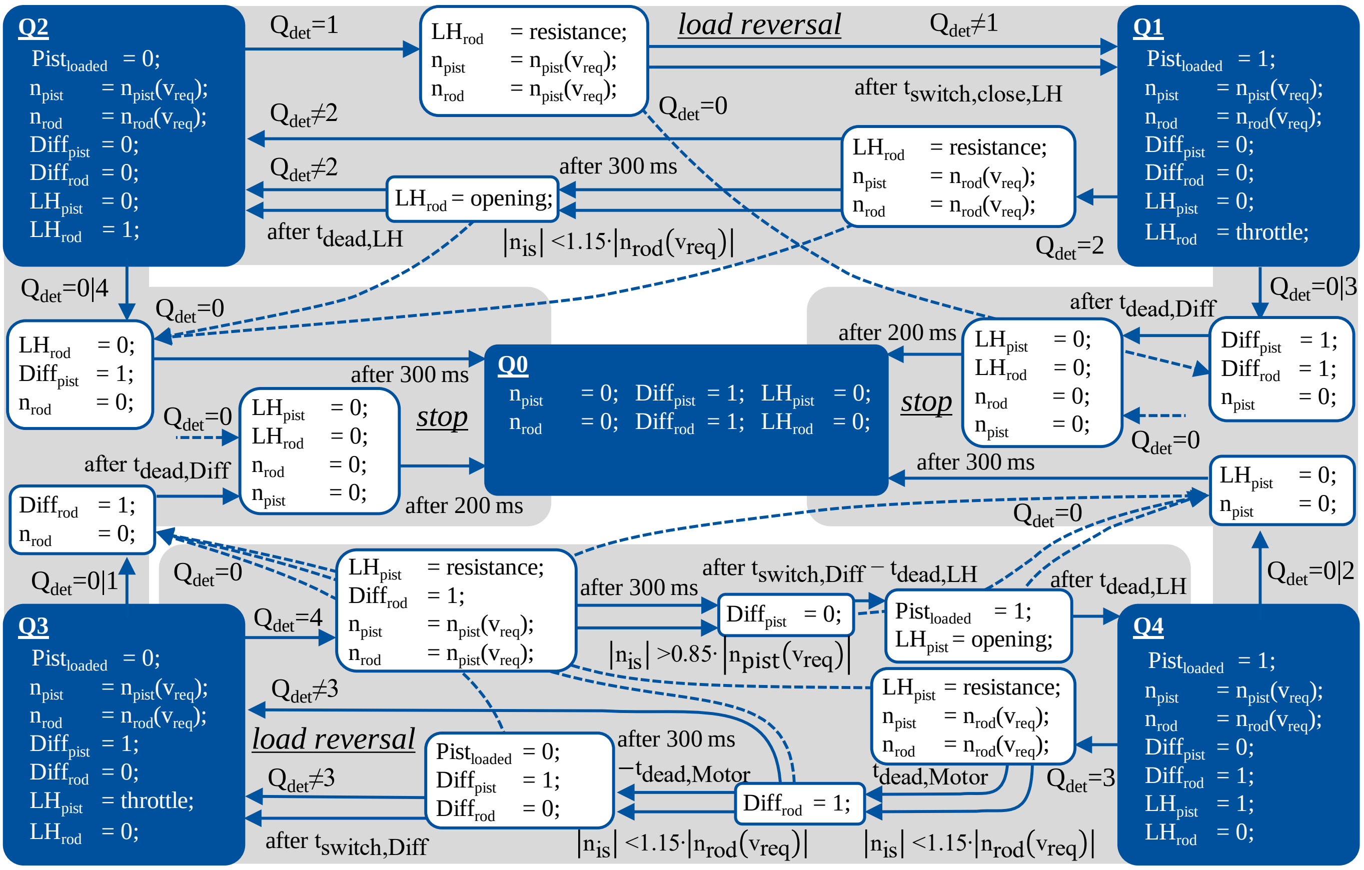

Figure 10: EHA controller – stopping and reversal of load direction

Looking at experimental data and considering the rough operation conditions of excavators, the authors assumed that small and short deviations can be accepted to a degree. This assumption must be experimentally verified in the future, since no meaningful metric could be found.

Lastly, the stopping of the EHA is mainly done by closing the load-holding valves. In case of a pumping operation, both pump ports are connected by additionally opening both differential valves. This results in fast depressurisation and energy cutoff. A stopping signal during any sequence will result in an immediate stop of the EHA. The dashed arrows in fig. 8 denoted with $Q_{det} = 0$ link to the equally marked arrows in fig. 10. On an additional note, changes between quadrants of the same kind (Q1↔Q3 & Q2↔Q4) are handled by first stopping and then accelerating again. The changes Q1↔Q3 occur frequently if the friction force dominates.

4 Simulation

In this chapter, the simulation design is briefly explained as well as the test cases used. Afterwards, the simulation results are introduced and discussed.

4.1 Design

The simulation approach was already described in [12]. The hydraulic circuit was modelled and parameterised in the lumped parameter fluid power simulation program DSHplus and exported as a functional mockup unit (FMU). It was then imported into Matlab Simulink, where the control was implemented. The most important simulation parameters are given in tab. 1. Sizing was done for a 1.8-ton excavator. The differential valves are modelled to have a linear opening characteristic and the load-holding valves are modelled as a first-order lag element. The sum of dead times and switching times is equal to the values taken from data sheets. Volumetric and hydromechanical efficiencies of the pump are based on a measured characteristic field. The cylinder friction is based on existing measurement data. The electric motor is of PMSM type and is modelled as shown in fig. 11. The model was aimed to include the reduction of torque at higher speeds. The maximum motor torque $M_{EM,max}$ as function of the rotational speed is therefore taken from the data sheet of the motor. Depending on the difference between requested speed n_{set} and current speed n, a PI-controller adjusts the applied motor torque M_{EM}. The acceleration is then calculated based on M_{EM}, the current motor load M_{load} as result of pressure difference and the moment of rotational inertia of the motor I_{EM} and pump I_P.

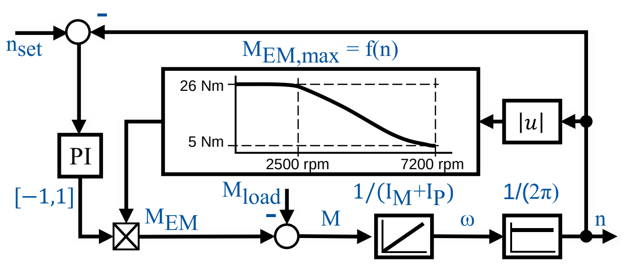

Figure 11: Simulation model of the PMSM

Table 1: Simulation parameters

Parameter	Value
pump displacement volume	5.4 cm^3
cylinder piston diameter	60 mm
cylinder rod diameter	35 mm
cylinder stroke	415 mm
cylinder equivalent mass	1000 kg
accumulator nominal volume	2 l
accumulator pre-charge pressure	4.5 bar
oil bulk modules at high pressures	14,000 bar
$t_{dead,Motor}$	50 ms
$t_{dead,Diff}$; $t_{dead,LH}$	20 ms
$t_{switch,Diff}$	40 ms
$t_{switch,\ open,LH}$	50 ms
$t_{switch,\ close,LH}$	150 ms
rotational acceleration limit	25,200 rpm/s
moment of inertia of motor and pump	0.011 kgm^2
$F_{Fric,static}$	250 N
$F_{Fric,base}$	0 N
$\dot{x}_{vis}$	50 mm/s
μ_{vis}	10 Ns/mm

The simulation allows investigation of the circuit behaviour for the testcases displayed in fig. 12. The velocity reversal case is used to investigate the corresponding quadrant changes by applying a constant force and changing the requested velocity direction. For the velocity reversal testcase, simulations were done for all combinations of force and velocity, since the velocity value correlates to the first request. Secondly, during the force reversal test case, the velocity is kept constant and the applied force is changed linearly. F_{mean} correlates roughly to the position of the hysteresis band. Therefore, the positive value is used for negative velocities and vice versa. It was adjusted to achieve the desired quadrant changes due to friction influences. Simulations were done for each combination of velocity and ΔF. The start position of the cylinder was set to 50 mm for positive velocities and 365 mm for negative velocities.

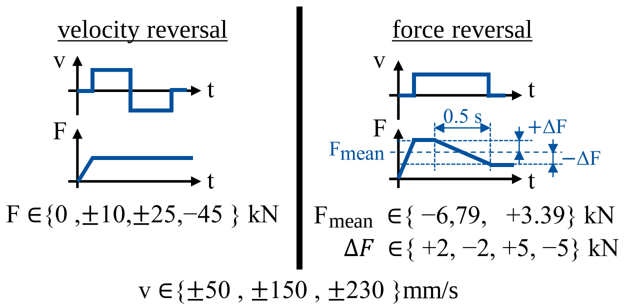

Figure 12: Test cases

4.2 Results

In this section, the simulation results for the introduced testcases of velocity and force reversal are shown and discussed.

4.2.1 Velocity reversal

Figure 13 shows the simulated cylinder velocities for the testcase in which the direction of cylinder movement is changed. The top side shows cases with a positive starting velocity and the bottom side with a negative. The shown timeframe excludes the initial load application. The requested velocity correlates with v_{req} in fig. 6 and therefore the change rate is not limited.

As shown in fig. 1, a negative external force corresponds to a force trying to push the cylinder inwards (Q1 & Q4). Looking at the velocities, one can see that the transitions from Q4→Q1 and Q2→Q3 are smooth and linear as designed. The transitions Q1→Q4 and Q3→Q2 show the designed rest close to zero velocity as shown in fig. 9 before accelerating again, noticeable by the offset between the lines above and below zero velocity. The influence of the reduced torque of the electric motor can be seen. It results in speed deviations for higher loads as well as reduced acceleration.

As explained earlier, at low external load conditions, the friction forces dominate, resulting in a quadrant change Q1↔Q3. Control-wise this is handled by a combination of stopping and accelerating, which clearly can be seen by looking at the 0 kN (black) lines. The velocity is reduced way quicker since the stopping is handled by closing the load-holding valves instead of slowing down the motor. To increase efficiency further, an additional sequence could be added that slows the cylinder down due to motor speed before then changing into the acceleration sequence.
Overall, the performance of the control is rated good. The transitions are smooth and there are only movements in the requested direction. The oscillations after stopping are a result of the quick stopping. The small oscillations during acceleration are assessed to be not noticeable during operation, since the operation conditions of mobile machinery are rough.

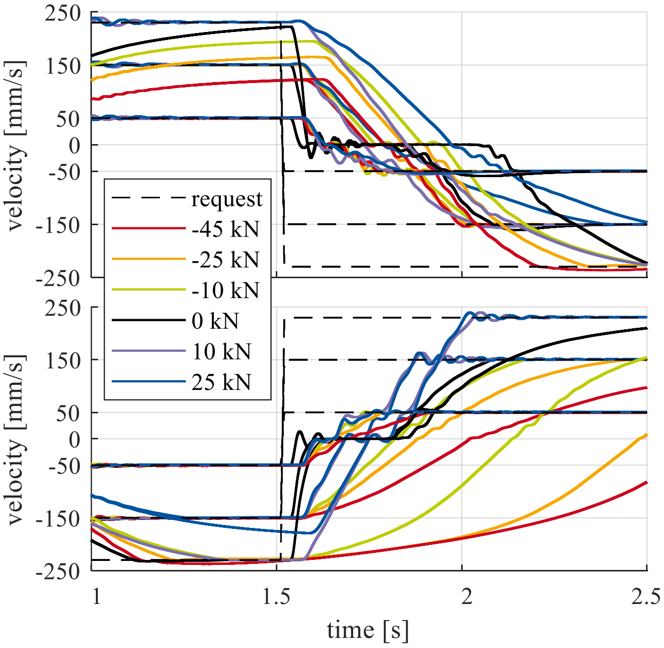

Figure 13: Results for the test case velocity reversal

4.2.2 Force reversal

Figure 14 shows, analogous to fig. 13, the simulated cylinder velocities for the different force combinations of the test case force reversal. The simulation results are sorted by the change of operating quadrant, resulting in four groups. The time when the quadrant change is detected is marked by a vertical line in the same colour as the corresponding velocity plot.

The topmost graph shows the change Q1→Q2. During the acceleration phase, small oscillations can be seen. Also, slower acceleration due to the reduced torque capacity of the electric motor at high speeds is visible as well. During the change, the motor speed needs to decrease to adjust to the smaller volume flow because of the smaller cylinder rod area. Looking at the timeframe in which the change occurs, only small deviations can be seen. The momentum of mass, assistive load and resistive valve mode keep the velocity close to the requested value. The initial overshoot at the higher load change rate is a result of the valve dynamics and the time needed to switch to resistive mode. The valve closes too slowly, so that the assistive load accelerates the cylinder. At lower change rates, the cylinder is still controlled by the pump speed if the rotational speed is reduced, resulting in a slowdown before valve control takes over. Looking at the requested velocities of 230 mm/s an oscillation is clearly visible. The motor speed does not match when the differential valve closes and results in an excitation of the system.

The second graph displays the results for the change Q2→Q1, in which the pump speed needs to increase. After the quadrant change is detected, the cylinder slows down due to friction and throttle pressure buildup. As soon as the pump volume flow matches the required cylinder volume flow, the pressure increases and the cylinder is controlled by the pump speed again. The switch back to pump control results in a small excitation. Higher change rates of load result in a faster slowdown. The pump speed adjusts fast enough to prevent large deviations at low speeds. At higher speeds, the reduced performance and larger speed adjustments increase the required timeframe, resulting in larger deviations.

The changes from Q3→Q4 are shown in the third graph. Analogue to Q2→Q1, the pump speed needs to increase during the change, but switches to motoring mode. At higher speeds, the pump speed does not match, resulting in a small excitation. The initial slowdown is a result of the pump rod side port being connected to the accumulator, removing the pushing force and the time required by the valve to switch to resistive mode. The valve dynamics explain the small overshoot afterwards as well, since the assistive load continues to increase.

Lastly the changes from Q4→Q3 are plotted in the downmost graph. Looking at the cylinder velocities, the worst performance of all quadrant changes can be seen. While changes at slower speeds show only small deviations they increase with increasing speeds. Further, a slower change rate of load initially results in acceleration due to a higher remaining load when the differential valve is opened. The valve must be opened, since otherwise the decrease of pump speed results in a slowdown of the cylinder because of the reduced flow. At -150 mm/s and -230 mm/s and -5 kN load change rate the cylinder slows down because the valve boundary is reached. Especially at -230 mm/s the pump speed adjustment is too slow.

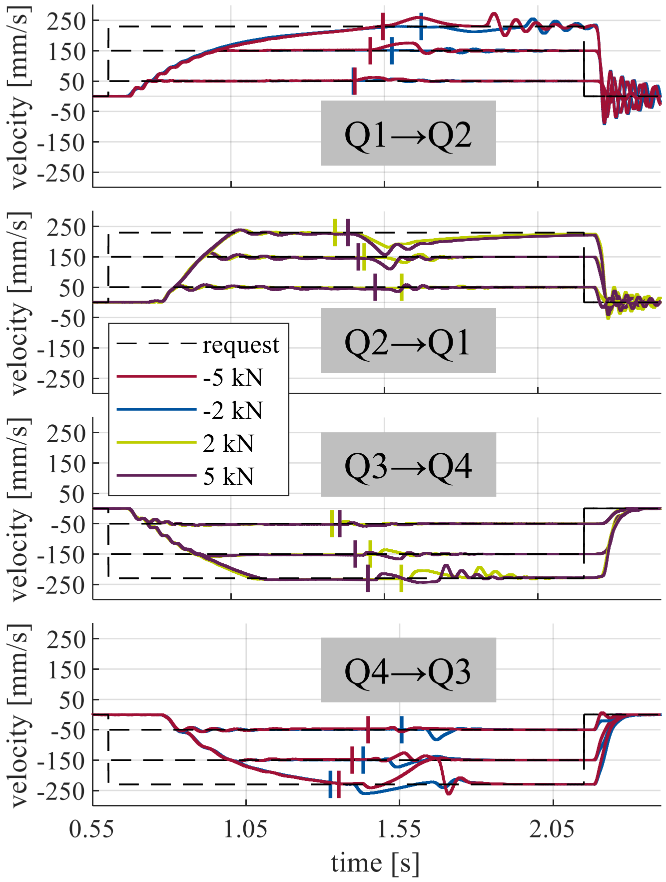

Figure 14: Results for testcase force reversal

Additionally, it can be observed that the valve-based stops result in strong oscillations after a movement in positive direction and a smooth deceleration after a movement in the negative direction. The reason for this is that the cylinder is under hydraulic tension while slowing down during inward movement. In Q4 the pump provides more fluid to the rod side than is required by the cylinder slowing down. The oversupply causes a pressure drop over the differential valve, tensioning the cylinder. The same is true for Q3 where the cylinder slows down faster than the pump because of the closing load-holding valve. The hydraulic tension prevents excitation of the system. In Q2 the pressure on the piston side of the cylinder is close to the accumulator pressure since the check valves are open. Only when the cylinder almost reaches zero velocity, the pump volume flow causes a small pressure buildup. The missing hydraulic tension results in a pressure buildup on the rod side due to the closing load-holding valve. The built-up pressure accelerates the cylinder inwards and results in oscillation. The same is true for Q1. The pressure does not drop to the accumulator pressure and is higher afterwards due to the faster pump speed. The oscillation is smaller as a result.

The duration of the cylinder velocity deviations is short and small, except for the change at higher speeds from Q4→Q3. If one considers that the reversal of external force represents a big change in operational conditions some acceptance for deviations by the operator is likely. For example, this occurs when ground excavation starts after lowering the arm in motor mode. Considering this, the shown velocity graphs are rated to be acceptable. Nevertheless, as already mentioned before, further research and experiments with human operators need to confirm this assessment.

5 Conclusion

In this paper, a hydraulic circuit for an electro-hydrostatic actuator (EHA) aimed at the application in mobile machinery is investigated. The circuit was selected based on cost considerations, the use of a high-speed internal gear pump and standard differential cylinder, inclusion of load-holding capability and wide flexibility of the control.
The boundaries for four-quadrant operation of this circuit are derived and explained. The existing boundaries require an extension of the pumping quadrant to allow full coverage of the four-quadrant plane. This is necessary since the operational conditions in mobile machinery are unpredictable and always changing. The extension is done by active throttling of the outgoing cylinder volume flow using proportional load-holding valves.
Based on the derived physical boundaries, a virtual boundary for the quadrant change is defined and combined with active hysteresis to prevent unwanted quadrant changes. The developed control scheme and controller architecture, mainly comprising two state machines, are presented. The controller aims to synchronise motor speed with valve positioning, allowing for smooth cylinder velocities under changing velocity requests and load directions.
The simulation results show good performance for the reversal of velocity under constant force. During the reversal of external load under constant speed, the deviations are higher but rated to be acceptable for the application in an excavator. The biggest deviations result from changes from Q4→Q3. Further, especially high speeds result in larger deviations because of the required adjustment of pump speed combined with reduced torque capacity of the electric motor.

6 Outlook

Experimental validation in an excavator with a human operator is recommended and planned. In future, the control scheme could be further refined and optimised. For example, an optimised pre-pressurisation during the acceleration sequence in motoring quadrants or a sequence allowing for recuperation during changes between quadrants Q1 and Q3 could be implemented. Additionally, a demonstrator of the EHA will be built and used to experimentally validate the simulation results.

Acknowledgements

The IGF research project "01IF22246N" of the research association Forschungskuratorium Maschinenbau e. V. – FKM, Lyoner Straße 18, 60528 Frankfurt am Main was supported from the budget of the Federal Ministry of Economic Affairs and Climate Action through the DLR within the scope of a program to support industrial community research and development (IGF) based on a decision of the German Bundestag.

Nomenclature

Designation	Denotation	Unit
A_{pist}, A_{rod}	Cylinder areas	m^2
$Diff_{pist/rod}$	Actuation of the switching valves	-
F	External cylinder force	N
F_{fric}	Friction force	N
$LH_{pist/rod}$	Mode of the load-holding valves	-
m	Equivalent mass	kg
n_{is}	Current rotational speed of the motor	min^{-1}
n_{min}	Minimal rotational speed of the pump	min^{-1}
$n_{pist/rod}$	rotational speed calculated by EHA controller if piston/rod side is loaded	min^{-1}
n_{thresh}	Threshold during a change of rotational direction	min^{-1}
p_{acc}	Accumulator pressure	bar
$p_{bound,acc}$	Load pressure boundary introduced by the accumulator pressure	bar
$p_{bound,fric}$	Load pressure boundary resulting from the cylinder friction	bar
$p_{bound,throttle}$	Load pressure boundary resulting from the throttling	bar
$p_{bound,valve}$	Load pressure boundary introduced by the load-holding valve	bar
p_{load}	Load pressure	bar
p_{rod}, p_{pist}	Cylinder pressures	bar
$p_{pump,rod/pist}$	Pressures at the pump ports	bar
$Pist_{loaded}$	Equal to 1, if piston side is loaded	-
POCV	Pilot-operated check valve	-
Δp_{Hyst}	Width of hysteresis	bar
$\Delta p_{throttle}$	Pressure difference while throttling	bar
Q	Volume flow	l/min
$Q0, Q1, Q2, Q3, Q4$	Operating quadrant in the four quadrant plane (Q0 = standstill)	-
Q_{det}	Output of quadrant detection	-
$t_{dead,LH}$	Dead time of load-holding valve	ms
$t_{dead,Diff}$	Dead time of switching valve	ms
$t_{dead,Motor}$	Dead time of motor	ms
$t_{switch,close,LH}$ $t_{switch,open,LH}$	Time to open/close the load-holding valve (incl. dead time)	ms
$t_{switch,Diff}$	Time to switch the position of the switching valve (incl. dead time)	ms
v_{req}	Requested cylinder velocity	m/s
$\dot{x}$	Cylinder velocity	m/s
α	Cylinder area ratio	-

References

[1] Williamson, C. and Ivantysynova, M., Stability and motion control of inertial loads with displacement controlled hydraulic actuators. *Proc. of 6th FPNI-PhD Symp.* West Lafayette, Indiana, June 15-19, 2010, S. 499–514.

[2] Michel, S., Elektrisch-hydrostatische Kompaktantriebe mit Differentialzylinder für die industrielle Anwendung, Dissertation, TU Dresden, Dresden, 2020. DOI 10.25368/2021.86.

[3] Williamson, C. and Ivantysynova, M., Pump mode prediction for four-quadrant velocity control of valveless hydraulic actuators. *Proc. of 7th JFPS International Symposium on Fluid Power.* Toyama, Japan, 15-18 September, 2008.

[4] Wang, L., Book, W. J., and Huggins, J. D., A Hydraulic Circuit for Single Rod Cylinders. In: *Journal of Dynamic Systems, Measurement, and Control*, Vol. 134, No. 1, 2012. DOI 10.1115/1.4004777.

[5] Çalışkan, H., Balkan, T., and Platin, B. E., A Complete Analysis and a Novel Solution for Instability in Pump Controlled Asymmetric Actuators. In: *Journal of Dynamic Systems, Measurement, and Control*, Vol. 137, No. 9, 2015. DOI 10.1115/1.4030544.

[6] Imam, A., Rafiq, M., Jalayeri, E., and Sepehri, N., Design, Implementation and Evaluation of a Pump-Controlled Circuit for Single Rod Actuators. In: *Actuators*, Vol. 6, No. 1, S. 10, 2017. DOI 10.3390/act6010010.

[7] Imam, A., Tolba, M. S., and Sepehri, N., Improving performance of pump-controlled hydraulic circuits for single-rod actuators: conceptual study. In: *Journal of Physics: Conference Series*, Vol. 2616, No. 1, S. 12015, 2023. DOI 10.1088/1742-6596/2616/1/012015.

[8] Koury Costa, G. and Sepehri, N., A Critical Analysis of Valve-Compensated Hydrostatic Actuators: Qualitative Investigation. In: *Actuators*, Vol. 8, No. 3, S. 59, 2019. DOI 10.3390/act8030059.

[9] Gøytil, P. H., Padovani, D., and Hansen, M. R., A Novel Solution for the Elimination of Mode Switching in Pump-Controlled Single-Rod Cylinders. In: *Actuators*, Vol. 9, No. 1, S. 20, 2020. DOI 10.3390/act9010020.

[10] Kärnell, S. and Ericson, L., Hysteresis Control in Pump-Controlled Systems—A Way to Reduce Mode-Switch Oscillations in Closed and Open Circuits. In: *Energies*, Vol. 15, No. 2, S. 424, 2022. DOI 10.3390/en15020424.

[11] Ketelsen, S., et al., Classification and Review of Pump-Controlled Differential Cylinder Drives. In: *Energies*, Vol. 12, No. 1293, 2019. DOI 10.3390/en12071293.

[12] Figge, F. and Schmitz, K., Simulative Comparison Approach of Electro-Hydrostatic Actuator Circuits in Excavators. *Proc. of ASME/BATH 2023 Symposium on Fluid Power and Motion Control.* Sarasota, Florida, USA, 16.-18. October, 2023. DOI 10.1115/FPMC2023-111798.

[13] Rahmfeld, R., Energy saving hydraulic actuators for mobile machines. *Proc. of 1st Bratislavian Fluid Power Symposium.* Casta-Pila, Slovakia, 2–3 June, 1998.

[14] Padovani, D., Ketelsen, S., Hagen, D., and Schmidt, L., A Self-Contained Electro-Hydraulic Cylinder with Passive Load-Holding Capability. In: *Energies*, Vol. 12, No. 292, 2019. DOI 10.3390/en12020292.

[15] Habibi, S. and Goldenberg, A., Design of a New High-Performance ElectroHydraulic Actuator. In: *IEEE/ASME TRANSACTIONS ON MECHATRONICS*, Vol. 5, No. 2, 2000.

[16] Michel, S. and Weber, J., Energy-efficient electrohydraulic compact drives for low power applications. *Proc. of Fluid Power and Motion Control FPMC 2012.* Bath, United Kingdom, 12-14 September, 2012.